High-Affinity Interactions of Tumor Necrosis Factor Receptor-Associated Factors (TRAFs) and CD40 Require TRAF Trimerization and CD40 Multimerization

Steven S. Pullen,[‡] Mark E. Labadia,[‡] Richard H. Ingraham,[‡] Sarah M. McWhirter,[§] Daniel S. Everdeen,[‡] Tom Alber,[§] James J. Crute,[‡] and Marilyn R. Kehry*[,‡]

Department of Biology, Boehringer Ingelheim Pharmaceuticals, Inc., Ridgefield, Connecticut 06877-0368, and Department of Molecular and Cell Biology, University of California, Berkeley, California 94720-3206

Received April 30, 1999; Revised Manuscript Received June 3, 1999

ABSTRACT: Signaling by some TNF receptor family members, including CD40, is mediated by TNF receptor-associated factors (TRAFs) that interact with receptor cytoplasmic domains following ligand-induced receptor oligomerization. Here we have defined the oligomeric structure of recombinant TRAF domains that directly interact with CD40 and quantitated the affinities of TRAF2 and TRAF3 for CD40. Biochemical and biophysical analyses demonstrated that TRAF domains of TRAF1, TRAF2, TRAF3, and TRAF6 formed homo-trimers in solution. N-terminal deletions of TRAF2 and TRAF3 defined minimal amino acid sequences necessary for trimer formation and indicated that the coiled coil TRAF-N region is required for trimerization. Consistent with the idea that TRAF trimerization is required for high-affinity interactions with CD40, monomeric TRAF-C domains bound to CD40 significantly weaker than trimeric TRAFs. In surface plasmon resonance studies, a hierarchy of affinity of trimeric TRAFs for trimeric CD40 was found to be TRAF2 > TRAF3 ≫ TRAF1 and TRAF6. CD40 trimerization was demonstrated to be sufficient for optimal NF-κB and p38 mitogen activated protein kinase activation through wild-type CD40. In contrast, a higher degree of CD40 multimerization was necessary for maximal signaling in a cell line expressing a mutated CD40 (T254A) that signaled only through TRAF6. The affinities of TRAF proteins for oligomerized receptors as well as different requirements for degree of receptor multimerization appear to contribute to the selectivity of TRAF recruitment to receptor cytoplasmic domains.

Tumor necrosis factor (TNF)[1] receptor-associated factors (TRAFs) interact with the cytoplasmic domains of many TNF receptor superfamily members, including TNFR2, CD40, CD30, LTβR, HVEM (ATAR), OX-40, and RANK (*1*−*3*). Receptor oligomerization with trimeric ligands is thought to initiate signaling by recruitment of TRAF proteins to receptor cytoplasmic domains. To date, six TRAF family members have been identified, and their functions are beginning to be elucidated. $CD8^+$ T cells from transgenic mice expressing TRAF1 are refractory to activation-induced cell death, implicating TRAF1 in regulating apoptosis (*4*). Genetic analyses have demonstrated TRAF2 is required for c-Jun N-terminal kinase (JNK) activation (*5, 6*). When overexpressed transiently in mammalian cells, TRAF2 also activates p38 mitogen activated protein kinase (MAPK) and nuclear factor-κB (NF-κB) (*7, 8*). Mice with a deletion of the TRAF3 gene have an impaired T cell-dependent immune response and display an early postnatal lethal phenotype (*9*). When transiently expressed in mammalian cells TRAF5 and TRAF6 mediate NF-κB and JNK activation (*10, 11*). TRAF6 also can induce extracellular signal-regulated kinase (ERK) (*10*) and p38 MAPK activation (*12*).

TRAF proteins can be subdivided into two functional domains. In the C-terminal half, or TRAF domain, a highly conserved C-terminal region (TRAF-C) mediates binding to receptor cytoplasmic domains and interactions with several other proteins such as NF-κB inducing kinase (NIK) and I-TRAF/TANK (*13*−*15*). The N-terminal region of the TRAF domain (TRAF-N) is a coiled coil that mediates interactions with c-IAP1, c-IAP2, Casper, and A20 (*16, 17*). The TRAF domain also mediates homo- and hetero-oligomerization (*2, 13, 18, 19*). The recent determination of the crystal structure of the TRAF domain of TRAF2 has demonstrated that it forms a trimer with both TRAF-N and TRAF-C domains contributing to the trimeric structure (*20, 21*). With the exception of TRAF1, all TRAFs contain a predicted RING and five or seven predicted zinc finger motifs N-terminal to the TRAF domain that are required for NF-κB and JNK activation (*11, 19, 22, 23*).

Because many TNF receptor superfamily members signal through similar subsets of TRAF proteins, it is important to understand how specificity is generated in TRAF-mediated signaling. An additional complexity in some receptors is the

* To whom correspondence should be addressed at Boehringer Ingelheim Pharmaceuticals, Inc., 900 Ridgebury Rd, P.O. Box 368, Mail code R6-5, Ridgefield, CT 06877-0368. Telephone: 203-791-6153. Fax: 203-791-6196. EMail: mkehry@bi-pharm.com.

[‡] Boehringer Ingelheim Pharmaceuticals, Inc.

[§] University of California.

[1] Abbreviations: TNF, tumor necrosis factor; TRAF, TNF receptor-associated factor; TNFR, TNF receptor; LTβR, lymphotoxin-β receptor; VEM (ATAR), herpesvirus entry mediator; NF-κB, nuclear factor κB; JNK, c-Jun N-terminal kinase; MAPK, mitogen-activated protein kinase; ERK, extracellular signal-regulated kinase; CD40c, CD40 cytoplasmic domain; GST, glutathione *S*-transferase; GST−CD40c, GST fusion protein with CD40c; IZip−CD40c, modified trimeric GCN4 isoleucine zipper−CD40c fusion protein; CD40L, CD40 ligand; sCD40L, soluble human CD40L; CD8α−CD40L, mouse CD8α−human CD40L fusion protein; PCR, polymerase chain reaction.

10.1021/bi9909905 CCC: $18.00
Published on Web 07/15/1999

presence of more than one TRAF binding site (CD40, CD30, and TRANCE/RANK) (*18, 24*−*26*). The CD40 receptor on antigen-presenting cells provides signals critical to propagation of T cell-dependent immune responses (*27*). Outcomes of CD40 signaling in B cells include induction of proliferation and differentiation and regulation of expression of surface proteins (*28*). The CD40 binding site for TRAF1, TRAF2, and TRAF3 has been mapped to the sequence ^{250}PVQET (*12, 18*). The TRAF6 binding site in CD40 is more membrane proximal, and has been mapped to the sequence ^{230}QEPQEINF (*12, 18*). In TNF receptor family members that bind TRAFs, each TRAF binding site, with the exception of the TRAF6 binding site, appears to interact with more than one TRAF (*1*−*3*). This implies that signals from a particular receptor are a composite of the interactions of multiple TRAFs and possibly competition among TRAFs. A hierarchy of affinities of different TRAFs for receptor binding sites also exists but has not been quantitated. This hierarchy appears to vary depending upon the receptor (*18, 25, 29, 30*).

Based on amino acid sequence homology of TRAF2 with other TRAFs, it has been suggested that all TRAF domains form homo-trimers (*20, 21*), but no studies have addressed the oligomeric composition of TRAFs other than TRAF2. Here we have overexpressed, isolated, and characterized the TRAF domain of each TRAF protein that directly interacts with human CD40, TRAF1, TRAF2, TRAF3, and TRAF6 (*18, 26*). Biochemical and biophysical analyses demonstrated that each TRAF domain existed as a trimer in solution. Binding studies indicated that TRAF trimerization was required for efficient interactions with CD40 while CD40 oligomerization also enhanced TRAF recruitment. TRAF6 appeared to require a greater extent of CD40 oligomerization for interaction and biological function. These findings suggest a general mechanism for generating specificity in receptor signaling through TRAF proteins.

MATERIALS AND METHODS

Plasmids and Viruses. A chimera with a coiled-coil trimerization domain was used to produce trimeric human CD40 cytoplasmic domain (CD40c). pCD40c (*18*) was digested with *Nco*I and *Eco*RI, and the CD40c-containing fragment was ligated into pET-23d (Novagen) at the same sites to make pET-23d/CD40c. The oligonucleotides 5′-CCCCTCTAGAAATAATTTTGTTTAACTTTAAG-3′, 5′-AAGGAGATATTACCATGAATCGTATCAAACAG-3′, 5′-ACTGAAGACAAAATCGAAGAAATCCTGTCCAA-3′, 5′-ACAGTACCACATCGAAAACGAAATCGCTCGTA-3′, 5′-TCAAGAAACTGATCGGTGAACGTTCCATGGA-3′, 5′-ATGGTAATATCTCCTTCTTAAAGTTAAACAAAA-TTATTTCTAGAGGGGA-3′, 5′-CGATTTTGTCTTCGAT-CTGTTTGATACGATTC-3′,5′-TTCGATGTGGTACTGTTT-GGACAGGATTTCTT-3′, and 5′-CCATGGAACGTTCAC-CGATCAGTTTCTTGATACGAGCGATTTCGTT-3′ were annealed and ligated to generate the trimeric pII variant of the GCN4 leucine zipper (IZip) (*31*). The ligated and gel-purified 160 bp DNA fragment was used as a PCR template with the oligonucleotides 5′-CCCCTCTAGAAATAATTT-TGTTTAACTTTAAGAA-3′ and 5′-GGCCATGGAACGT-TCACCGATCAGTTTCTTGATACGAGCG-3′, and ligated into pCR2.1 (InVitrogen) to make pCR2.1/IZip. The plasmid pCR2.1/IZip was digested with *Xba*I and *Nco*I, and the fragment was ligated into pET-23d/CD40c to make pET-23d/IZip−CD40c.

To produce soluble trimeric human CD40L (sCD40L), DNA encoding the TNFα homologous portion of the human CD40 ligand extracellular domain (amino acids Gly^{116} through Leu^{261}) (*32, 33*) was PCR-amplified from a full-length cDNA clone (K. Kishimoto, K. Meek, P. Lipsky, and M. R. Kehry, unpublished results) using the oligonucleotides 5′-GGTTGGTTCATATGGGTGATCAGAATCCT-CAAATTGC-3′ and 5′-CCAACCAAGCGGCCGCTTAT-CAGAGTTTGAGTAAGCCAAAGGA-3′. The resulting 473 bp PCR product was digested with *Nde*I and *Not*I and cloned into the same sites of pET20b(+) (Novagen) to generate pET20b/CD40L.

The oligonucleotides 5′-CCATGGGAGTGCTCATCTG-GAAGATTCGCGA-3′ and 5′-GAATTCTCATCAGGGATCG-GGCAGATCCG-3′ were used to PCR amplify the TRAF3-C domain (encoding amino acids 416−568), from pGemT/TRAF3 (*18*), and the fragment was ligated into pCR2.1 to make pCR2.1/TRAF3-C. The plasmid pCR2.1/TRAF3-C was digested with *Nco*I and *Eco*RI, and the TRAF3 fragment was ligated into pVL1393/Flag (*18*) to generate pVL1393/FlagTRAF3-C. The plasmid pVL1393/FlagTRAF3-C was digested with *Nco*I and *Not*I, and the TRAF3-C fragment was ligated into pET-23d/IZip−CD40c to make pET-23d/IZip−TRAF3-C. pET-23d/IZip−TRAF3-C was digested with *Not*I and partially digested with *Xba*I, and the 654 bp IZip−TRAF3-C fragment was ligated into pVL1393 (InVitrogen) to generate pVL1393/IZip−TRAF3-C. The 5′ oligonucleotides 5′-CCATGGCCCAAGACAAGATTGAAGCCC-TGAGTAGC-3′ and 5′-CCATGGCCAGGAGCATTGGC-CTCAAGGACCTG-3′ and the 3′ oligonucleotide 5′-GAAT-TCTTTGCCTCCATCTTGGAGAC-3′ were used to PCR amplify fragments of TRAF2, from the plasmid pVL1393/TRAF2-CA21 (*18*), which were ligated into pCR2.1 to make pCR2.1/TRAF2-Q311 and pCR2.1/TRAF2-R326, respectively. The *Nco*I−*Eco*RI fragments from pCR2.1/TRAF2-Q311 and pCR2.1/TRAF2-R326 were ligated into pVL1393/TRAF2-NC-CA21 and pVL1393/FlagTRAF2-NC (*18*) to make pVL1393/TRAF2-NC-Q311-CA21 (encoding amino acids 311−501 of TRAF2 with a C-terminal CA21 epitope tag) and pVL1393/FlagTRAF2-NCR326 (encoding amino acids 326−501 of TRAF2), respectively. The recombinant baculovirus stocks AcMNPV/Flag-TRAF3-C, AcMNPV/IZip−TRAF3-C, AcMNPV/TRAF2-NC-Q311-CA21, and AcMNPV/Flag-TRAF2-NC-R326 were generated by standard methods (*34*) from the transplacement vectors described above. Viruses AcMNPV/Flag-TRAF1-NC, AcMNPV/Flag-TRAF2-NC, AcMNPV/Flag-TRAF3-NC, and AcMNPV/Flag-TRAF6-NC have been described previously (*18*).

Protein Expression and Isolation. Expression of CD40c and IZip−CD40c in *E. coli* strain BL21(DE3) was induced with 1.0 mM IPTG for 3 h at 37 °C. Harvested cell paste was resuspended in 2 volumes of lysis buffer (20 mM HEPES, pH 7.5, 200 mM NaCl, 1 mM DTT, 1 mM EDTA, 1 mM EGTA, 10% v/v glycerol, 1 mM PMSF, 4 μg/mL leupeptin, 4 μg/mL pepstatin A), frozen by pipetting into liquid nitrogen, and stored at −80 °C. Thawed cell paste was resuspended in an equal volume of lysis buffer, and cells were disrupted by nitrogen cavitation. Extracts were clarified by ultracentrifugation for 75 min at 100000*g*. Saturated ammonium sulfate was added to 66% v/v at 4 °C, and

precipitated proteins were resuspended in buffer A (20 mM HEPES, pH 7.0, 1 mM DTT, 10% v/v glycerol, 0.1 mM EDTA, 0.1 mM EGTA, and 1 mM PMSF) with 200 mM NaCl. The NaCl concentration was adjusted to 100 mM, and the sample was applied to a Source 15S column (Amersham Pharmacia Biotech) equilibrated in buffer A with 80 mM NaCl. Proteins were eluted with a 100 mM to 1.1 M NaCl gradient in buffer A. Peak fractions were chromatographed through Sephacryl S-300 HR equilibrated in buffer A containing 300 mM NaCl. Purified protein was quantitated using a Micro BCA assay (Pierce Chemical Co.) relative to GST−CD40c (*18*) as a standard, and stored at −80 °C.

Expression of sCD40L in *E. coli* BL21(DE3)pLysS was induced with 0.5 mM IPTG for 3 h at 25 °C, and the cell paste was harvested, frozen under liquid nitrogen, and stored at −80 °C. Frozen cell paste was resuspended in 20 mM BisTris, pH 6.8, 100 mM NaCl, 5 mM EDTA, 1 mM DTT, 10% glycerol (5 mL/1 g of cells). Cells were lysed on ice by sonication, and the lysate was centrifuged at 20000*g* for 30 min at 4 °C. One tenth volume of 0.5% poly(ethylenimine), pH 7.9, was added dropwise to the supernatant with stirring at room temperature. The lysate was centrifuged at 100000*g* for 75 min at 4 °C, filtered through a 0.2 μM filter, and applied to a Poros 20 HS cation exchange column (PerSeptive Biosystems) equilibrated in 25 mM MES, pH 6.4, 1 mM EDTA, 1 mM DTT, 5% glycerol. The column was washed with equilibration buffer and eluted with a linear gradient of 0−1.0 M NaCl in equilibration buffer. The sCD40L peak was chromatographed on a Sephacryl S-100 HR column (Amersham Pharmacia Biotech) in equilibration buffer containing 150 mM NaCl. Fractions containing sCD40L were pooled, filtered through a 0.2 μM filter, quantitated (*35*), and stored at 4 °C. Purified sCD40L was characterized by analytical ultracentrifugation and found to be a noncovalent trimer (49 830 Da by sedimentation equilibrium and 49 020 Da by sedimentation velocity analyses; data not shown).

Spodoptera frugiperda (Sf21) cells were maintained and infected as described previously (*36*) using medium supplemented with 5% heat-inactivated fetal bovine serum (HyClone) and 50 μg/mL gentamicin sulfate (Life Technologies, Inc.). All purification procedures for protein expressed in Sf21 cells were performed at 4 °C. Cytosolic extracts of baculovirus-infected Sf21 cells were prepared as described (*18*, *36*). Saturated ammonium sulfate was added to 43% v/v for Flag-TRAF2-NC-R326 and TRAF2-NC-Q311-CA21 and to 33% for Flag-TRAF1-NC, Flag-TRAF3-NC, and Flag-TRAF3-C. Precipitated proteins were resuspended in buffer A with 200 mM NaCl. The NaCl concentration was adjusted to 100 mM, and the sample was applied to coupled Source 15S and Source 15Q columns (Amersham Pharmacia Biotech) equilibrated in buffer A with 80 mM NaCl. The flow-through was applied to a Ceramic Hydroxyapatite (type II) column (BioRad) equilibrated in 50 mM potassium phosphate, pH 6.2, 100 mM NaCl, 0.2 mM DTT. For Flag-TRAF1-NC, Flag-TRAF2-NC-R326, Flag-TRAF3-C, and Flag-TRAF3-NC, proteins were eluted with a 50−275 mM potassium phosphate, pH 6.2, gradient. For TRAF2-NC-Q311-CA21, flow-through from the Ceramic Hydroxyapatite column was adjusted to 1.1 M ammonium sulfate and applied to a Phenyl-Superose column (Amersham Pharmacia Biotech) equilibrated in 50 mM postassium phosphate, pH 6.2, 1.1 M ammonium sulfate, 1.0 mM DTT, and proteins were eluted with a 1.1−0 M ammonium sulfate gradient in 50 mM postassium phosphate, pH 6.2, 20% glycerol, 1.0 mM DTT. Cytosolic extracts containing Flag-TRAF2-NC or Flag-TRAF6-NC were applied to an anti-Flag M2 affinity column (Kodak) equilibrated in buffer A with 150 mM NaCl. After washing with buffer A containing 400 mM NaCl, Flag-TRAF2-NC was eluted with 50% ImmunoPure Gentle Ag/Ab Elution Buffer (Pierce)/50% buffer A containing 400 mM NaCl without DTT. Flag-TRAF6-NC was eluted in buffer A with 150 mM NaCl and 250 μg/mL Flag peptide (Kodak). All proteins were chromatographed through Sephacryl S-300 HR (Amersham Pharmacia Biotech) equilibrated in buffer A with 300 mM NaCl. Glycerol and PMSF were omitted from samples used in surface plasmon resonance studies. Purified proteins were quantitated as described (*35*) and stored at −80 °C.

To purify IZip−TRAF3-C, the nuclear fraction from baculovirus-infected Sf21 cells was prepared as described (*36*), without the addition of ATP or $MgCl_2$, and an equal volume of cell lysis buffer containing 10% w/v sucrose was added. An equal volume of buffer A, pH 7.5, with 800 mM NaCl was added and incubated at 4 °C for 10 min. Extracts were clarified by ultracentrifugation at 100000*g*; proteins were precipitated with saturated ammonium sulfate (66% v/v) at 4 °C, and resuspended in buffer A, pH 7.5, with 200 mM NaCl. The sample was applied to and eluted from a Source 15S column as described above. IZip−TRAF3-C was applied to a 5D10 anti-IZip affinity column (CNBr-activated Sepharose 4B; Amersham Pharmacia Biotech) equilibrated in 20 mM HEPES, pH 7.5, 150 mM NaCl. The column was washed using 20 mM HEPES, pH 7.5, 500 mM NaCl and eluted using ImmunoPure Gentle Ag/Ab Elution Buffer (Pierce). Purified protein was dialyzed using buffer A, pH 7.5 without DTT or glycerol, with 300 mM NaCl, quantitated as described (*35*), and stored at −80 °C. Mouse CD8α−human CD40 ligand (mCD8α−hCD40L) was expressed and purified as described previously (*12*). The molecular mass of purified mCD8α−hCD40L as determined by analytical ultracentrifugation analysis was consistent with a minimally glycosylated hexamer or heptamer (data not shown).

Anti-IZip Production. BALB/c mice were immunized intraperitoneally with 100 μg of purified IZip−CD40c fusion protein (*37*). Mice received the first immunization in complete Freund's adjuvant and three subsequent immunizations in incomplete Freund's adjuvant. One animal with a high-titer serum was boosted with 50 μg of IZip−CD40c in PBS intravenously 4 days before spleen cell fusion to the P3X63Ag8.653 myeloma (*38*−*40*). Clone 5D10, a mouse IgG1/κ, was one of two positive clones selected from the initial screening and was subcloned twice by limiting dilution. The final subclone 5D10.3B3.7C10 was shown to be free of *Mycloplasma* contamination and was used for all further antibody preparations. The 5D10 antibody was purified as described (*41*).

TRAF Cross-Linking. Five micrograms of each TRAF domain protein was mock-treated or treated with a final concentration of 0.1% or 0.01% glutaraldehyde in 50 μL of 25 mM potassium phosphate, pH 8.0, for 1 h at room temperature. Samples were mixed with an equal volume of 2% SDS, 50 mM Tris-HCl, pH 6.8, and 2% 2-ME and heated

at 95 °C for 5 min. Portions were analyzed by SDS−PAGE (12% polyacrylamide Tris−glycine; Novex) followed by staining with Coomassie Brilliant Blue R350.

Coupled Size Exclusion Chromatography−Laser Light Scattering. The molecular mass of purified proteins was determined using size exclusion chromatography on a Hewlett-Packard HP1090 Chemstation with in-line detection using a Wyatt Mini-Dawn laser light scattering detector and a Waters 410 Differential Refractometer. Bio-Silect columns (BioRad), either 400-5 in tandem with a 250-5 or a 250-5 alone, were used with running buffer (20 mM TES, pH 7.0, 0.3 M NaCl). Protein concentrations were calculated using a d*n*/d*c* value of 0.185. Laser light scattering data were analyzed using Astra software version 4.5 (Wyatt Technology Corp.).

Analytical Ultracentrifugation. Experiments were performed using a Beckman Model XL-1 analytical ultracentrifuge using either two-sector cells (sedimentation velocity) or six-hole cells (sedimentation equilibrium). Sedimentation equilibrium analyses were in 20 mM TES, pH 7.0, 0.2 M NaCl, 1 mM DTT at 20 °C and used rotor speeds of 20 000, 25 000, 30 000, and 35 000 rpm at three concentrations. Data were edited and analyzed using the programs REEDIT, NonLin, and Noneq4 (*42*, *43*) provided by the National Analytical Ultracentrifugation Facility at the University of Connecticut, Storrs, CT.

Sedimentation velocity analyses were performed at 50 000 or 55 000 rpm at 20 °C in 20 mM TES, pH 7.0, 0.3 M NaCl. Predicted partial specific volumes (ν) and hydration parameters (δ) were calculated using Sednterp ver. 1.00 (*44*, *45*). Global nonlinear least-squares fitting of the data was performed using the program Svedberg ver. 5.01 [provided by Dr. J. S. Philo (*44*)].

TRAF Binding Assays. GST coprecipitation assays were as described previously using purified GST−CD40c (20 μg; 590 pmol), purified TRAF protein (1000 pmol), and 10 μL of glutathione Sepharose 4B (Amersham Pharmacia Biotech) (*18*). Solid-phase TRAF−CD40c ELISA was as described previously (*12*). Plates were probed with 2 μM purified TRAF protein, and binding was detected with 1.0 μg/mL anti-Flag BioM2 antibody (Kodak) and streptavidin−horseradish peroxidase (0.5 μg/mL; Jackson ImmunoResearch).

Surface Plasmon Resonance Analyses. All experiments were performed on a BIACORE 1000 (Biacore, Inc.). IZip−CD40c or CD40c was immobilized on a BIAcore CM5 sensor chip using amine-coupling (EDC) as recommended by the manufacturer. Subsequently, the surface was blocked with an 8 min injection of 1 M ethanolamine. Surface densities of immobilized ligands ranged from 150 to 300 resonance units. Surface K_D measurements were obtained by performing direct binding assays. Briefly, dilutions of TRAF proteins were prepared in running buffer (50 mM HEPES, pH 7.0, 100−300 mM NaCl, 0.1 mM EDTA, 0.1 mM EGTA, 1 mM DTT) and injected over the surface at a flow rate of 15 μL/min. Data were collected from the equilibrium portion of all sensorgrams, and binding isotherms were generated using SAS (version 6.1) (*46*).

Cellular Signaling Assays. NF-κB reporter assays were as described previously (*12*). Cells were stimulated for 6 h with 10 μg/mL sCD40L or 10 μg/mL mCD8α−hCD40L. p38 MAPK activation assays were as described previously (*12*). Cells were stimulated for 15 min with 10 μg/mL sCD40L or 10 μg/mL mCD8α−hCD40L.

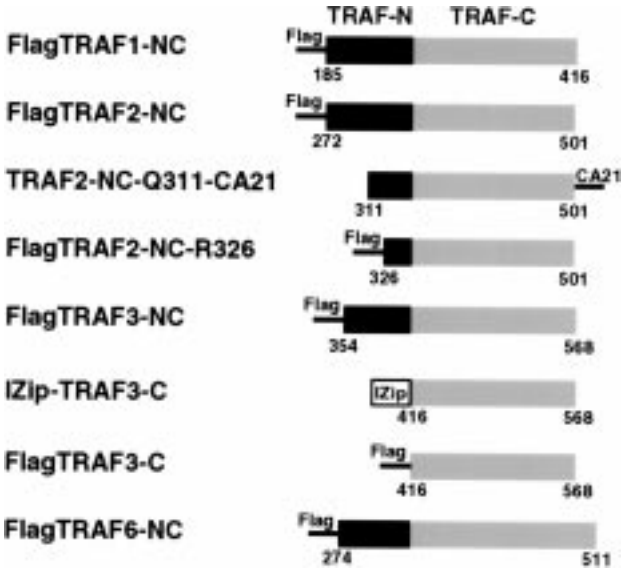

FIGURE 1: Recombinant TRAF domains. The TRAF-N domain (black), the TRAF-C domain (gray), and the modified isoleucince zipper (white, IZip) are represented to scale for each protein. The N-terminal and C-terminal amino acid positions for each protein as well as the N-terminal Flag and C-terminal CA21 epitope tags are indicated.

RESULTS

Oligomeric Structure of the TRAF Domain. To study the oligomeric structures of TRAF1, TRAF2, TRAF3, and TRAF6 and their interactions with CD40, eight TRAF domain constructs (Figure 1) were expressed in insect cells. Each protein was purified to near-homogeneity, and the identity was verified by electrospray ionization mass spectrometry (Table 1). Each of the Flag-tagged proteins was N-terminally acetylated, and TRAF2-NC-Q311-CA21 lacked the N-terminal Met and was acetylated on the next amino acid residue (Ala). No other covalent modifications were detected.

Several approaches were used to define the oligomeric structure of the TRAF domain of TRAF1, TRAF3, and TRAF6. Initially, low concentrations of purified TRAF domains were cross-linked with two different concentrations of glutaraldehyde. After analysis by SDS−PAGE, oligomers of Flag-TRAF1-NC, TRAF2-NC-Q311-CA21, and Flag-TRAF3-NC with mobilities consistent with cross-linked dimers and trimers were evident. Dimers and trimers increased relative to monomer with increasing glutaraldehyde concentration (Figure 2, lanes 3, 6, 12). Cross-linked multimers of Flag-TRAF6-NC were also present but could not be resolved into distinct species due to cross-linking with minor copurifying proteins. After glutaraldehyde cross-linking, Flag-TRAF2-NC also formed distinct dimers and trimers similar to TRAF2-NC-Q311-CA21 (data not shown).

Laser light scattering was used to calculate a molecular mass for all purified TRAF domains (Table 1). These results were consistent with each TRAF-NC domain existing as a trimer in solution (TRAF2-NC-Q311-CA21, Flag-TRAF3-NC, and Flag-TRAF6-NC; Table 1). Only Flag-TRAF1-NC exhibited a molecular mass higher than expected for a trimer. This result was probably due to the poor solubility of this

Table 1: Biophysical Analyses of TRAFs

protein	M^a	M (predicted trimer)	M_r(light scat.)^b	M_r(sed. vel.)^c	M_r(sed. eq.)^d
Flag-TRAF1-NC	27 991	83 973	105 700	81 150	ND
TRAF2-NC-Q311-CA21	23 074	69 222	74 820	71 040	63 686
Flag-TRAF2-NC-R326	21 682	65 046	27 190	18 340	30 289
Flag-TRAF3-NC	26 046	78 138	78 260	74 470	73 431
Flag-TRAF3-C	19 050	57 150	22 740	19 510	19 488
Flag-TRAF6-NC	30 504	91 512	110 600	86 590	ND
CD40c	6 932	NA^e	ND^e	8 140	6 921
IZip−CD40c	11 402	34 206	ND	32 640	ND

[a] Molecular mass in Da as determined by electrospray ionization mass spectrometry. [b] Molecular mass in Da as determined by size exclusion chromatography−laser light scattering as described under Materials and Methods. [c] Molecular mass in Da as determined by sedimentation velocity analysis as described under Materials and Methods. [d] Molecular mass in Da as determined by sedimentation equilibrium analysis as described under Materials and Methods. [e] ND, not determined; NA, not applicable.

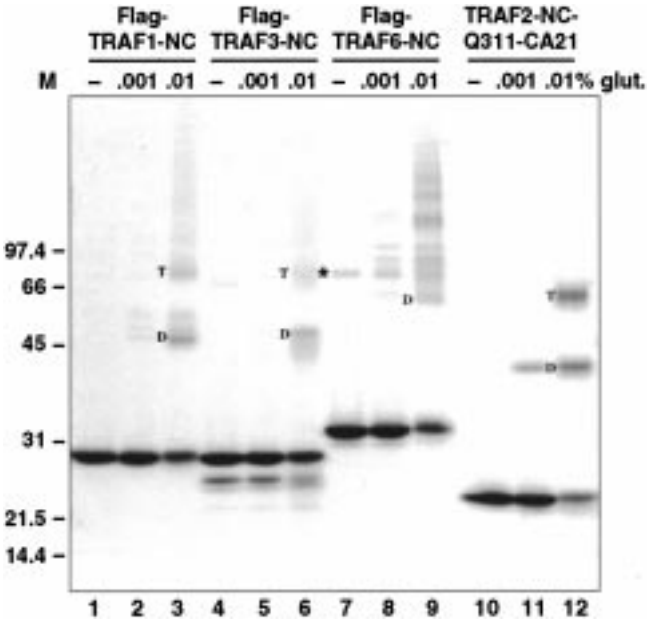

FIGURE 2: Glutaraldehyde cross-linking of TRAF domains. Purified TRAF domains were either untreated (−) or treated with the indicated percentage of glutaraldehyde. Proteins were separated by SDS−PAGE on a 12% polyacrylamide gel and visualized by staining with Coomassie Brilliant Blue. Migration positions of dimeric (D) and trimeric (T) TRAF oligomers are indicated. Molecular mass markers (M) listed in kDa. The asterisk indicates a contaminating protein that copurified with Flag-TRAF6-NC.

polypeptide and its tendency to precipitate. Sedimentation equilibrium and sedimentation velocity experiments further confirmed the composition of each TRAF-NC protein as a trimer (Table 1). We then tested the effect of removing most or all of the N-domain. In contrast to proteins containing the entire TRAF domain, Flag-TRAF3C appeared to be a monomer as determined by laser light scattering and analytical ultracentrifugation analyses (Table 1). Flag-TRAF2-NC-R326 was a monomer at low protein concentrations, but it formed a fraction of trimers at higher protein concentrations (Table 1; data not shown). These results indicate that the TRAF domains of TRAF1, TRAF2, TRAF3, and TRAF6 exist as homo-trimers. The TRAF-N domains of TRAF2 and TRAF3 are required for trimer formation.

Interactions of CD40 with TRAF Domains. To examine the requirement for TRAF trimerization in receptor binding, each purified TRAF domain protein was tested for interactions with a GST−CD40c fusion protein. In coprecipitation experiments, the trimeric proteins Flag-TRAF1-NC, Flag-TRAF2-NC, TRAF2-NC-Q311-CA21, and Flag-TRAF6NC interacted efficiently with GST-CD40c (Figure 3A). However, Flag-TRAF2-NC-R326 and Flag-TRAF3-C interacted weakly with GST−CD40c. None of the purified TRAF proteins interacted with GST alone (*18*; data not shown), demonstrating the specificity of the interactions. To better quantitate the interactions of trimeric and monomeric TRAFs with CD40, a solid-phase TRAF binding assay was used. In this assay, TRAF concentration was kept constant at 2 μM, and GST−CD40c fusion protein was titrated over a broad concentration range to allow detection of low-affinity interactions. Flag-TRAF2-NC-R326 and Flag-TRAF3-C bound poorly, if at all, to GST−CD40c when compared to Flag-TRAF2-NC and Flag-TRAF3-NC, respectively (Figure 3B). Sedimentation equilibrium analyses (Table 1) predict that at 2 μM Flag-TRAF2-NC-R326 was predominantly monomer. These data suggest that TRAF trimerization is required for higher affinity interactions of TRAFs with CD40c.

To confirm that the TRAF-N domain serves to trimerize TRAFs and is not involved in making contacts with CD40c or otherwise structuring the TRAF-C domain, TRAF3-C was engineered as a trimer by the N-terminal addition of a coiled-coil trimerization domain (IZip−TRAF3-C). Analytical ultracentrifugation of IZip−TRAF3-C demonstrated that it was a trimer (data not shown). In coprecipitation experiments, IZip−TRAF3-C bound to GST−CD40c as efficiently as Flag-TRAF3-NC (Figure 4), indicating that the TRAF3-N domain is required for trimerizing the TRAF3-C domain and serves primarily to increase the avidity of interactions with CD40c.

Surface plasmon resonance studies were performed to determine affinities of trimeric TRAF domain proteins for the CD40 cytoplasmic domain. The ligand for CD40 is known to be a trimer (*47*). By analogy to the structure of TNF receptor 1 bound to LT-α (*48*), it is assumed that CD40L engagement results in at least trimerization of CD40. To simplify measurements of molecular interactions between trimeric TRAF proteins and ligand-bound CD40, a locked trimeric CD40c was engineered by attaching IZip to the N-terminus of CD40c (IZip−CD40c). Purified IZip−CD40c formed a trimer as confirmed by analytical ultracentrifugation (Table 1). TRAF2-NC-Q311-CA21 bound IZip−CD40c with a surface K_D of 2.5 μM (Figure 5). The CA21 epitope tag did not affect the binding of TRAF2-NC-Q311-CA21 since the same protein without the epitope tag had a similar affinity (K_D = 3 μM, data not shown). Flag-TRAF3-NC bound to IZip−CD40c with an approximately 5-fold lower affinity (K_D = 13 μM), consistent with previous studies suggesting that

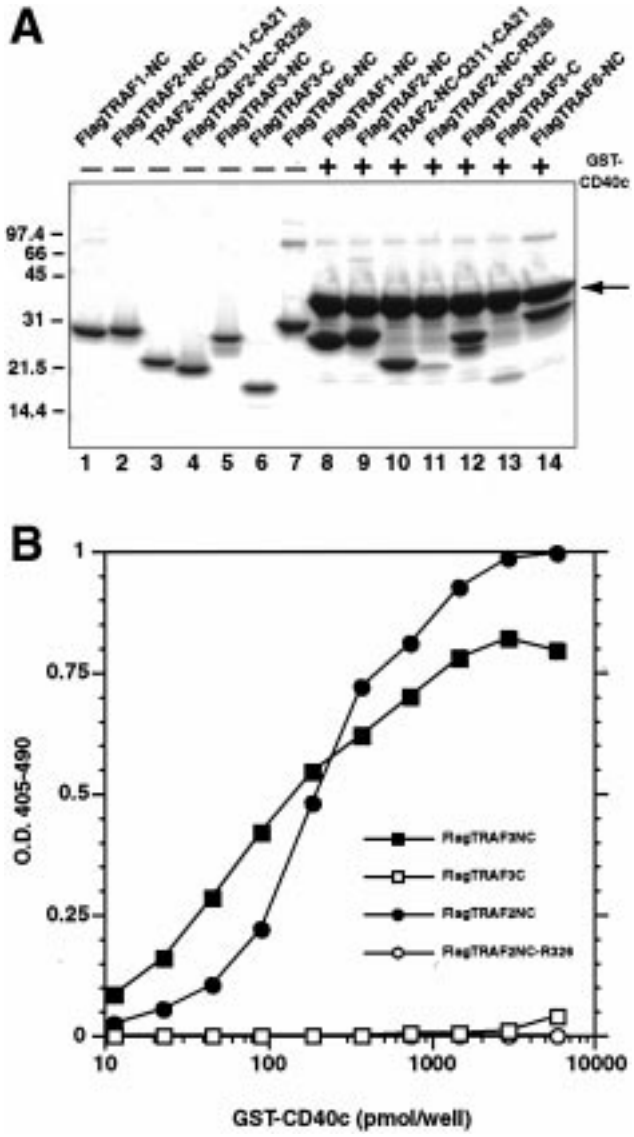

FIGURE 3: In vitro association of TRAF proteins with the CD40 cytoplasmic domain. (A) GST coprecipitation assays were performed using 20 μg of GST−CD40c, 1 μmol of TRAF protein, and 10 μL glutathione Sepharose 4B. Lanes 1−7, 10% of each input TRAF protein (−) used in coprecipitations. Lanes 8−14, GST−CD40c coprecipitations (+) with the indicated purified TRAF proteins. Precipitated proteins were separated by SDS−PAGE on a 16% polyacrylamide gel and visualized by staining with Coomassie Brilliant Blue. The arrow indicates the position of GST−CD40c. (B) Solid-phase binding assay for GST−CD40c−TRAF interaction. Purified TRAF proteins (2 μM each) were incubated in wells containing serial dilutions of purified GST−CD40c and detected with biotinylated anti-Flag BioM2 antibody and streptavidin−HRP. No signal was generated in the assay when GST alone was tested for TRAF binding or with anti-Flag BioM2 antibody in the absence of TRAF protein (data not shown). Each point is the mean of duplicate wells. Representative of two independent experiments.

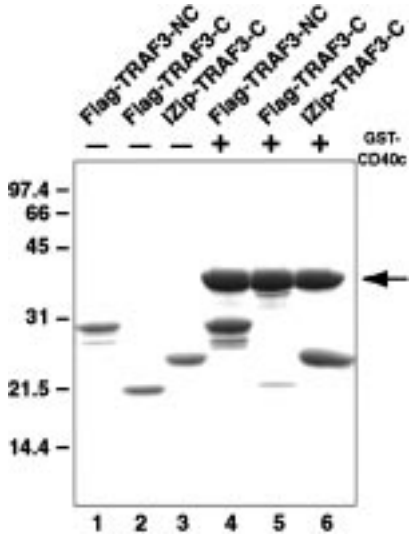

FIGURE 4: In vitro association of IZip−TRAF3-C with the CD40 cytoplasmic domain. GST coprecipitation assays were performed as described in the Figure 3 legend. Lanes 1−3, 10% of each input TRAF protein (−) used in coprecipitations. Lanes 4−6, GST−CD40c coprecipitations (+) with the indicated purified TRAF proteins. Precipitated proteins were separated by SDS−PAGE on a 16% polyacrylamide gel and visualized by staining with Coomassie Brilliant Blue. The arrow indicates the position of GST−CD40c. No binding of IZip−TRAF3-C was found when GST alone was tested (data not shown).

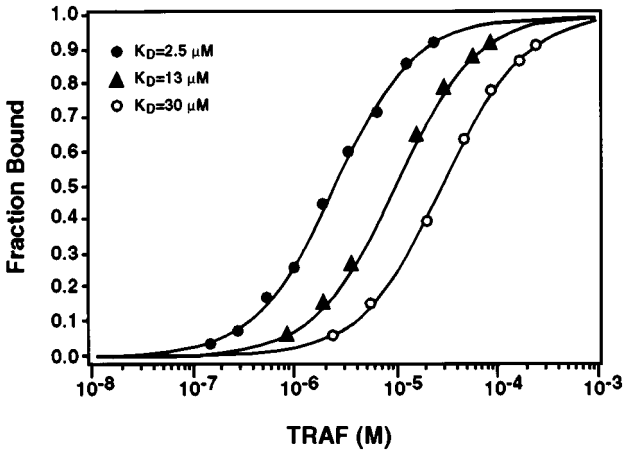

FIGURE 5: Surface plasmon resonance analysis of TRAF2-NC and TRAF3-NC interaction with CD40c. Immobilization of CD40c (open circles) or IZip−CD40c (closed triangles and closed circles) to a BIAcore sensor chip was done to obtain ~300 RU of signal. The indicated monomer concentrations of TRAF domains were used for injection. CD40c−TRAF2-NC-Q311-CA21 binding, open circles; IZip−CD40c−Flag-TRAF3-NC binding, closed triangles; IZip−CD40c−TRAF2-NC-Q311-CA21 binding, closed circles. Calculated surface K_D values for each isotherm are listed. No TRAF binding was detected using control surfaces. Each experiment shown is representative of three independent experiments. Each point is the mean of duplicates.

full-length TRAF3 binds to CD40c more weakly than TRAF2 (*18*). Using 51 or 316 μM solutions of Flag-TRAF1-NC or Flag-TRAF6-NC, respectively, no specific binding to IZip−CD40c could be detected (data not shown). Due to the poor solubility of Flag-TRAF1-NC, higher concentrations could not be tested. These results are consistent with previous results that showed full-length TRAF1 and TRAF6 bind more poorly to the CD40 cytoplasmic domain than TRAF2 and TRAF3 (*18*).

CD40 receptor on antigen-presenting cells is engaged by transiently expressed CD40L on the surface of activated T cells. Interactions of numerous other receptors and ligands occur between these two cell surfaces. Most of the engaged receptor−ligand pairs have been found to colocalize to the area of cell-cell contact to form a two-dimensional network (*49, 50*). In this context of two interacting cell surfaces, it is likely that CD40 engaged by CD40L also forms a higher order oligomeric network. To investigate the role of CD40

multimerization in mediating TRAF recruitment, we used surface plasmon resonance to compare TRAF binding to monomeric CD40 (CD40c) and trimeric CD40 (IZip−CD40c). TRAF2-NC-Q311-CA21 bound to CD40c with a 12-fold lower affinity than to IZip−CD40c trimers (K_D = 30 μM; Figure 5). These results demonstrated that CD40 trimerization increased the avidity of TRAF2 for CD40c. Because no binding of Flag-TRAF6-NC to IZip−CD40 was detected in the surface plasmon resonance analyses under conditions used with TRAF2 and TRAF3, a higher surface density of IZip−CD40c was tested for TRAF6 binding. Flag-TRAF6-NC at 316 μM was observed to bind specifically to a 10-fold higher density of IZip−CD40c (data not shown). It was not possible to obtain a quantitative K_D value due to the high quantity and concentrations of Flag-TRAF6-NC required. This suggested that a higher degree of CD40 multimerization than trimerization may be required for TRAF6 interactions.

Dependence of CD40 Signaling on the Extent of CD40 Multimerization. It is known that signaling through CD40 results in activation of NF-κB (*51, 52*) and that both TRAF1/2/3 and TRAF6 binding sites in CD40 are required for maximal activation (*12, 53, 54*). The ability of different extents of CD40 multimerization to mediate NF-κB activation was tested in cells. Purified recombinant soluble trimeric CD40L (sCD40L) and soluble hexameric CD40L (mCD8α−hCD40L) were characterized by analytical ultracentrifugation to confirm subunit structures (see Materials and Methods). These reagents were used to cross-link CD40 to differing extents on the surface of two stably transfected human embryonic kidney (HEK) 293 cell lines. One transfectant expressed wild-type CD40, and the other expressed a CD40 mutant (T254A) that has a single amino acid alteration in the TRAF1/2/3 binding site (^{250}PVQET) that eliminates TRAF1/2/3 binding. The CD40 T254A mutant appears to signal only through TRAF6 (*12*). NF-κB activation was quantitated by transfecting cells with an NF-κB reporter plasmid and stimulating cells with either sCD40L trimer or mCD8α−hCD40L hexamer. Cells expressing wild-type CD40 had higher basal levels of NF-κB activity than cells expressing CD40 T254A, as previously demonstrated (*12*) (Figure 6A). sCD40L and mCD8α−hCD40L stimulated similar levels of NF-κB activation in cells expressing wild-type CD40. In cells expressing CD40 T254A, sCD40L trimer stimulated low levels of NF-κB activation. mCD8α−hCD40L hexamer mediated a 7-fold greater increase in NF-κB activity than sCD40L (Figure 6A). These results indicate that CD40 trimerization was sufficient for maximal NF-κB activation through wild-type CD40 that had an intact TRAF1/2/3 binding site. However, a greater degree of CD40 multimerization was required for maximal NF-κB activation mediated through TRAF6 binding in the absence of TRAF2 and TRAF3 binding.

Previous studies have demonstrated that CD40 signaling activates p38 MAPK (*55, 56*) and that TRAF6 contributes significantly (*12*). The effect of CD40 multimerization on activation of p38 MAPK in wild-type CD40 and CD40 T254A-expressing HEK 293 cell lines was also examined. Similar basal levels of active p38 MAPK were detected in wild-type CD40 and CD40 T254A-expressing HEK 293 cell lines (Figure 6B) as well as in untransfected HEK 293 cells (*12*). Wild-type CD40 transfectants showed a similar increase

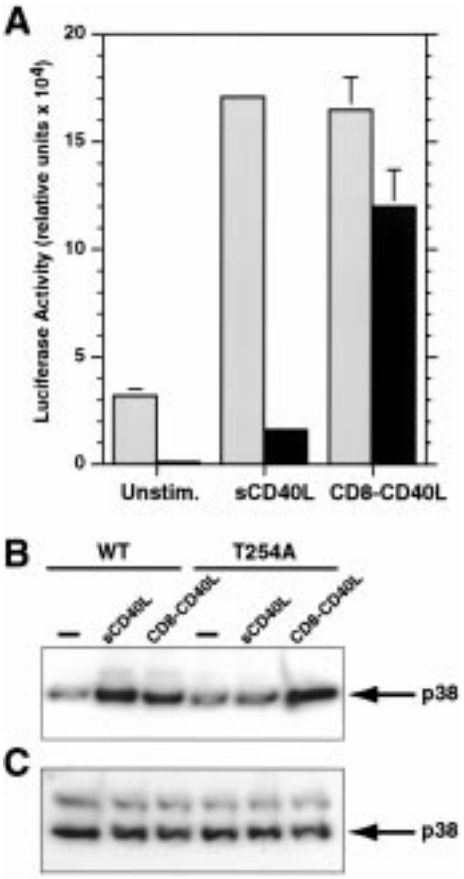

FIGURE 6: CD40 signaling depends on CD40L multimerization. (A) CD40-mediated NF-κB activation. Stably transfected HEK 293 cell lines expressing wild-type CD40 (gray) or CD40 T254A (black) were transfected with a NF-κB−luciferase reporter plasmid and stimulated for 6 h with medium, sCD40L (10 μg/mL) or mCD8α−hCD40L (10 μg/mL), and lysates were assayed for luciferase activity. Results are mean ± standard deviation of triplicate transfections. (B, C) CD40-mediated p38 MAPK activation. Lysates were prepared from stably transfected HEK 293 cell lines expressing wild-type CD40 or the CD40 T254A mutation 15 min after either mock-stimulation (−) or stimulation with sCD40L (10 μg/mL) or mCD8α−hCD40L (10 μg/mL). Proteins in each lysate were separated by SDS−PAGE on a 12% polyacrylamide gel and electroblotted to a PVDF membrane. Detection of phosphorylated active p38 MAPK (B) and total p38 (C) protein was performed by immunoblotting as described under Materials and Methods.

in active p38 MAPK levels following sCD40L or mCD8α−hCD40L treatment. Cells expressing CD40 T254A that lacks TRAF1/2/3 binding showed no increase in active p38 MAPK after treatment with sCD40L trimer. However, treatment of CD40 T254A cells with mCD8α−hCD40L hexamer caused a significant increase in activated p38 MAPK levels. As a control, in both cell lines, similar levels of total active and inactive p38 MAPK were present (Figure 6C). These results are consistent with the biochemical data presented above that suggest a higher degree of CD40 multimerization than trimerization is required for signaling mediated through TRAF6 binding.

DISCUSSION

Previous studies demonstrated that the TRAF domain of TRAF proteins mediates homo- and hetero-oligomerization (*13, 18, 19*) and that the TRAF domain of TRAF2 is a trimer (*20, 21*). Here we have delineated the oligomeric composition

of the TRAF domains of TRAF1, TRAF3, and TRAF6 and biochemically characterized the role of oligomerization in TRAF binding to CD40. Chemical cross-linking, laser light scattering, and analytical ultracentrifugation demonstrated that the TRAF domains of TRAF1, TRAF2, TRAF3, and TRAF6 form homo-trimers in solution (Figure 2 and Table 1). Additional experiments on the recombinant TRAF domain of TRAF4 also indicated that TRAF4 forms trimers in solution (data not shown). Consistent with crystallographic results on TRAF2 (*20, 21*), a portion of the TRAF-N domain of TRAF2 and TRAF3 was required for trimer formation. Thirty-nine amino acids could be deleted from the N-terminus of the TRAF2-N domain to generate trimeric TRAF2-NC-Q311. However, deletion of 15 additional TRAF-N domain amino acids to generate TRAF2-NC-R326 or removal of all of the TRAF-N domain of TRAF3 (TRAF3-C) resulted in proteins that were predominantly monomers at concentrations where the full-length TRAF domains were trimers (2 μM). TRAF2-NC-R326 formed trimers only at higher protein concentrations (50 μM), indicating that deleting residues 311−325 of TRAF2 destabilized trimers. Previous studies are also consistent with our findings. The TRAF2-N domain (272−358) and TRAF2-C domain (355−501) were shown not to form hetero-oligomers with full-length TRAF2 (*19*). In a previous study of TRAF3, amino acids 340−568 self-associated, whereas amino acids 389−568 did not (*57*). Together these results support the inference that intermolecular contacts observed in the TRAF2 crystal structure in both the TRAF-N coiled-coil domain and the TRAF-C domain contribute to trimerization of TRAFs (*20, 21*). Our findings suggest that this overall trimeric structure would be conserved among all six TRAF proteins.

Trimeric TRAF domains of TRAF2 and TRAF3 interacted efficiently with CD40; however, monomeric TRAF-C domains interacted weakly with CD40 (Figure 3). Consistent with these findings, a previous study showed the TRAF3-C domain (amino acids 389−568) interacted poorly with lymphotoxin-β receptor (LTβR) (*57*). An engineered TRAF3-C trimer formed by complete replacement of the TRAF3-N domain bound as efficiently to CD40 as the wild-type TRAF3-NC (Figure 4). This confirms that the TRAF3-N domain is involved in trimerization but not in receptor binding or in otherwise structuring the TRAF-C domain for receptor binding. In contrast to our findings, previous yeast two-hybrid studies have shown the TRAF2-C domain (344−501) and the TRAF3-C domain (415−568) interact with the cytoplasmic domains of CD30 and CD40, respectively (*58, 59*). This apparent discrepancy could be explained by quantitative differences and differences in the dynamic range between in vitro binding assays and yeast two-hybrid analyses.

Our studies suggest that TRAF trimerization appears to be required for efficient interactions with receptor cytoplasmic domains. We predict that full-length TRAFs would need to be preassembled as at least trimers in order to be effectively recruited following receptor engagement. It remains to be determined whether full-length TRAFs are preformed trimers in cells. The requirement for TRAF trimerization in receptor engagement suggests possible mechanisms for turning off TRAF signaling. In addition to competition for receptor binding sites, signaling could be inhibited by destabilization of TRAF trimerization. Any mechanism that reduced the concentration of functional TRAF trimers, including phosphorylation, proteolysis (*60, 61*), or regulatory protein binding to TRAF monomers, would be expected to reduce signaling.

Each TNF receptor family member ligand that has been expressed and purified as a soluble molecule is a trimer (*33, 47*). By analogy with the structure of the LTβ−TNFR1 complex (*48*), TNF receptors are expected to trimerize following engagement with their cognate ligands. As suggested by the structure of TRAF2 (*20, 21*), a geometric match between extracellular and intracellular ligands provides mechanisms for discrimination and stabilization of ligand-bound trimeric receptors by TRAFs. Thus, avidity-driven recruitment of TRAF complexes to the receptor cytoplasmic domains could initiate intracellular signaling cascades. This idea is specifically supported by our findings that the affinity of trimeric TRAFs for receptors is inherently low and that CD40 receptor trimerization was required for higher affinity interactions with trimeric TRAF2 (Figure 5). These data also are consistent with previous studies in cells that demonstrate TRAFs associate with receptor cytoplasmic domains following receptor cross-linking (*61, 62*).

A more quantitative hierarchy of CD40−TRAF affinities was also established using surface plasmon resonance studies. The K_D of TRAF3 interaction with trimeric CD40c was 13 μM, a 5-fold lower affinity than TRAF2 for CD40c (Figure 5). TRAF1 binding to trimeric CD40c could not be demonstrated at 51 μM, and, similarly, TRAF6 binding to trimeric CD40c could not be demonstrated at 316 μM. These experiments set lower limits on the respective K_D values and suggest that TRAF1 and TRAF6 bind to CD40c with at least 20-fold and 125-fold lower affinities than TRAF2, respectively. The quantitation of a hierarchy of affinities of TRAFs for CD40 supports the idea that the relative levels of TRAFs in a particular cell type would determine which TRAFs preferentially bind and signal. Levels of TRAF mRNA in cells have been found to be upregulated by certain stimuli, including CD40 ligation (*55, 63*). It would be expected that this would contribute significantly to regulating the CD40 responsiveness of cells in different activation states and in establishing selectivity in signaling by different TNF receptors.

Because specific TRAF6 binding to a higher density of trimeric CD40 was observed in surface plasmon resonance analyses, this suggested that a higher degree of CD40 multimerization could be required for recruitment of TRAF6. Alternatively, since the TRAF6 binding site in IZip−CD40c is situated closer to the coiled coil (*18*), the IZip−CD40c may not provide optimum geometry for TRAF6 interaction. Therefore, the effect of degree of CD40 multimerization on TRAF6 interaction was examined in a cellular system using a mutant CD40 receptor that only interacts with TRAF6 (CD40 T254A) (*12*). The celluar results demonstrated that the CD40 T254A receptor signaled only when ligated with hexameric CD40L and not with trimeric CD40L (Figure 6). Thus, initiation of CD40 signaling through TRAF6 may require more extensive CD40 multimerization by CD40L. Consistent with these results is the possibility that TRAF2 and TRAF3 could promote TRAF6 binding by further multimerizing CD40 following engagement with CD40L. These results also are consistent with studies in B cells demonstrating that different degrees of CD40 cross-linking

result in different cellular responses (*64*). Particular cellular responses requiring higher degrees of receptor multimerization, such as induction of proliferation or cytokine production, may be mediated by CD40 through TRAF6.

These studies extend initial findings from the crystal structure of TRAF2 by biochemically characterizing TRAF1, TRAF3, and TRAF6 TRAF domains as trimeric proteins at much lower concentrations than used in the crystallographic work. The trimeric architecture of TRAFs and ligand-bound receptors establishes a role for trimerization in initiating signaling. Similar mechanisms as described here for CD40 would be expected to regulate the interactions of TRAFs with other TNF receptor family members and establish selectivity in signaling. It remains to be determined whether other signaling proteins that interact with TRAFs (e.g., TRADD, I-TRAF/TANK, cIAP-1, cIAP-2, etc.) also form trimers or oligomers to promote assembly of signaling complexes.

ACKNOWLEDGMENT

We thank Heather White for help cloning TRAF2-NC-Q311-CA21 and Flag-TRAF2-NC-R326, Lee Frego and Walter Davidson for mass spectrometry analysis, Maurice Morelock for help graphing surface plasmon resonance data, Anita Wayne for generating hybridoma cell lines, Thu Dang for screening hybridoma cell lines, and Dr. John Miglietta, Anthony Shrutkowski, and Gale Hansen for DNA sequencing analysis.

REFERENCES

1. Baker, S. J., and Reddy, E. P. (1998) *Oncogene 17*, 3261−3270.
2. Arch, R. H., Gedrich, R. W., and Thompson, C. B. (1998) *Genes Dev. 12*, 2821−2830.
3. Gravestein, L. A., and Borst, J. (1998) *Semin. Immunol. 10*, 423−434.
4. Speiser, D. E., Lee, S. Y., Wong, B., Arron, J., Santana, A., Kong, Y. Y., Ohashi, P. S., and Choi, Y. (1997) *J. Exp. Med. 185*, 1777−1783.
5. Lee, S. Y., Reichilin, A., Santana, A., Sokol, K. A., Nussenzweig, M. C., and Choi, Y. (1997) *Immunity 7*, 703−713.
6. Yeh, W. C., Shahinian, S., Speiser, D., Kraunus, J., Billia, F., Wakeham, A., de la Pompa, J. L., Ferrick, D., Betty, H., Iscove, N., Ohashi, P., Rothe, R., Goeddel, D. V., and Mak, T. W. (1997) *Immunity 7*, 715−725.
7. Carpentier, I., Declercq, W., Malinin, N. L., Wallach, D., Fiers, W., and Beyaert, R. (1998) *FEBS Lett. 425*, 195−198.
8. Rothe, M., Sarma, V., Dixit, V. M., and Goeddel, D. V. (1995) *Science 269*, 1424−1427.
9. Xu, Y., Cheng, G., and Baltimore, D. (1996) *Immunity 5*, 407−415.
10. Kashiwada, M., Shirakata, Y., Inoue, J., Nakano, H., Okazaki, K., Okumura, K., Yamamoto, T., Nagaoka, H., and Takemori, T. (1998) *J. Exp. Med. 187*, 237−244.
11. Song, H. Y., Regnier, C. H., Kirschning, C. J., Goeddel, D. V., and Rothe, M. (1997) *Proc. Natl. Acad. Sci. U.S.A. 94*, 9792−9796.
12. Pullen, S. S., Dang, T. T. A., Crute, J. J., and Kehry, M. R. (1999) *J. Biol. Chem. 274*, 14246−14254.
13. Rothe, M., Wong, S. C., Henzel, W. J., and Goeddel, D. V. (1994) *Cell 78*, 681−692.
14. Cheng, G., and Baltimore, D. (1996) *Genes Dev. 10*, 963−973.
15. Malinin, N. L., Boldin, M. P., Kovalenko, A. V., and Wallach, D. (1997) *Nature 385*, 540−544.
16. Rothe, M., Pan, M. G., Henzel, W. J., Ayres, T. M., and Goeddel, D. V. (1995) *Cell 83*, 1243−1252.
17. Shu, H. B., Halpin, D. R., and Goeddel, D. V. (1997) *Immunity 6*, 751−763.
18. Pullen, S. S., Miller, H. G., Everdeen, D. S., Dang, T. T. A., Crute, J. J., and Kehry, M. R. (1998) *Biochemistry 37*, 11836−11845.
19. Takeuchi, M., Rothe, M., and Goeddel, D. V. (1996) *J. Biol. Chem. 271*, 19935−19942.
20. McWhirter, S. M., Pullen, S. S., Holton, J. M., Crute, J. J., Kehry, M. R., and Alber, T. (1999) *Proc. Natl. Acad. Sci. U.S.A. 96*, 8408−8413.
21. Park, Y. C., Burkitt, V., Villa, A. R., Tong, L., and Wu, H. (1999) *Nature 398*, 533−538.
22. Reinhard, C., Shamoon, B., Shyamala, V., and Williams, L. T. (1997) *EMBO J. 16*, 1080−1092.
23. Liu, Z. G., Hsu, H., Goeddel, D. V., and Karin, M. (1996) *Cell 87*, 565−576.
24. Wong, B. R., Josein, R., Lee, S. Y., Vologodskaia, M., Steinman, R. M., and Choi, Y. (1998) *J. Biol. Chem. 273*, 28355−28359.
25. Gedrich, R. W., Gilfillan, M. C., Duckett, C. S., Van Dongen, J. L., and Thompson, C. B. (1996) *J. Biol. Chem. 271*, 12852−12858.
26. Ishida, T., Mizushima, S., Azuma, S., Kobayashi, N., Tojo, T., Suzuki, K., Aizawa, S., Watanabe, T., Mosialos, G., Kieff, E., Yamamoto, T., and Inoue, J. (1996) *J. Biol. Chem. 271*, 28745−28748.
27. Kawabe, T., Naka, T., Yoshida, K., Tanaka, T., Fujiwara, H., Suematsu, S., Yoshida, N., Kishimoto, T., and Kikutani, H. (1994) *Immunity 1*, 167−178.
28. Foy, T. M., Aruffo, A., Bajorath, J., Buhlmann, J. E., and Noelle, R. J. (1996) *Annu. Rev. Immunol. 14*, 591−617.
29. Marsters, S. A., Ayres, T. M., Skubatch, M., Gray, C. L., Rothe, M., and Ashkenazi, A. (1997) *J. Biol. Chem. 272*, 14029−14032.
30. Devergne, O., Hatzivassiliou, E., Izumi, K. M., Kaye, K. M., Kleijnen, M. F., Kieff, E., and Mosialos, G. (1996) *Mol. Cell. Biol. 16*, 7098−7108.
31. Harbury, P. B., Kim, P. S., and Alber, T. (1994) *Nature 371*, 80−83.
32. Hollenbaugh, D., Grosmaire, L. S., Kullas, C. D., Chalupny, N. J., Braesch-Andersen, S., Noelle, R. J., Stamenkovic, I., Ledbetter, J. A., and Aruffo, A. (1992) *EMBO J. 11*, 4313−4321.
33. Eck, M. J., and Sprang, S. R. (1989) *J. Biol. Chem. 264*, 17595−17605.
34. O'Reilly, D. R., Miller, L. K., and Luckow, V. A. (1992) *Baculovirus expression vectors: a laboratory manual*, W. H. Freeman & Co., Salt Lake City, UT.
35. Gill, S. C., and von Hippel, P. H. (1989) *Anal. Biochem. 182*, 319−326.
36. Dracheva, S., Koonin, E. V., and Crute, J. J. (1995) *J. Biol. Chem. 270*, 14148−14153.
37. Lane, P., Brocker, T., Hubele, S., Padovan, E., Lanzavecchia, A., and McConnell, F. (1993) *J. Exp. Med. 177*, 1209−1213.
38. Kearney, J. F., Radbruch, A., Liesegang, B., and Rajewsky, K. (1979) *J. Immunol. 123*, 1548−1550.
39. Harlow, E., and Lane, D. (1988) *Antibodies: A laboratory manual*, Cold Spring Harbor Press, Cold Spring Harbor, NY.
40. Springer, T. A. (1985) *Hybridoma Technology in the Biosciences and Medicine*, Plenum Press, New York.
41. Hardy, R. R. (1986) *Handbook of Experimental Immunology*, Vol. 13.1−13.13, Blackwell Scientific Publications, Cambridge, MA.
42. Johnson, M. L., Correia, J. J., Yphantis, D. A., and Halvorson, H. R. (1981) *Biophys. J. 36*, 575−588.
43. Awakawa, T., and Yphantes, D. A. (1987) *J. Biol. Chem. 262*, 7484−7485.
44. Philo, J. S. (1994) in *Modern Analytical Ultracentrifugation, Acquisition and Interpretation of Data for Biological and Synthetic Polymer Systems*, Birkhauser Publishing, Inc., Boston, MA.
45. Laue, T. M., Shah, B. D., Ridgeway, T. M., and Pelletier, S. L. (1994) in *Analytical Ultracentrifugation in Biochemistry and Polymer Science*, The Royal Society of Chemistry, Cambridge, England.

46. Morelock, M. M., Ingraham, R. H., Betageri, R., and Jakes, S. (1995) *J. Med. Chem. 38*, 1309−1318.
47. Karpusas, M., Hsu, Y. M., Wang, J. H., Thompson, J., Lederman, S., Chess, L., and Thomas, D. (1995) *Structure 3*, 1031−1039.
48. Banner, D. W., D'Arcy, A., Janes, W., Gentz, R., Schoenfeld, H. J., Broger, C., Loetscher, H., and Lesslauer, W. (1993) *Cell 73*, 431−445.
49. Kupfer, A., and Singer, S. J. (1988) *Proc. Natl. Acad. Sci. U.S.A. 85*, 8216−8220.
50. Monks, C. R., Freiberg, B. A., Kupfer, H., Sciaky, N., and Kupfer, A. (1998) *Nature* 395, 82−86.
51. Berberich, I., Shu, G. L., and Clark, E. A. (1994) *J. Immunol. 153*, 4357−4366.
52. Francis, D. A., Karras, J. G., Ke, X. Y., Sen, R., and Rothstein, T. L. (1995) *Int. Immunol. 7*, 151−161.
53. Ishida, T., Kobayashi, N., Tojo, T., Ishida, S., Yamamoto, T., and Inoue, J. (1995) *J. Immunol. 155*, 5527−5535.
54. Hsing, Y., Hostager, B. S., and Bishop, G. A. (1997) *J. Immunol. 159*, 4898−4906.
55. Craxton, A., Shu, G., Graves, J. D., Saklatvala, J., Krebs, E. G., and Clark, E. A. (1998) *J. Immunol. 161*, 3225−3236.
56. Salmon, R. A., Foltz, I. N., Young, P. R., and Schrader, J. W. (1997) *J. Immunol. 159*, 5309−5317.
57. Force, W. R., Cheung, T. C., and Ware, C. F. (1997) *J. Biol. Chem. 272*, 30835−30840.
58. Lee, S. Y., Lee, S. Y., Kandala, G., Liou, M. L., Liou, H. C., and Choi, Y. (1996) *Proc. Natl. Acad. Sci. U.S.A. 93*, 9699−9703.
59. Cheng, G., Cleary, A. M., Ye, Z. S., Hong, D. I., Lederman, S., and Baltimore, D. (1995) *Science 267*, 1494−1498.
60. Duckett, C. S., and Thompson, C. B. (1997) *Genes Dev.* 11, 2810−2821.
61. Kuhne, M. R., Robbins, M., Hambor, J. E., Mackey, M. F., Kosaka, Y., Nishimura, T., Gigley, J. P., Noelle, R. J., and Calderhead, D. M. (1997) *J. Exp. Med. 186*, 337−342.
62. VanArsdale, T. L., VanArsdale, S. L., Force, W. R., Walter, B. N., Mosialos, G., Kieff, E., Reed, J. C., and Ware, C. F. (1997) *Proc. Natl. Acad. Sci. U.S.A. 94*, 2460−2465.
63. Wang, C. Y., Mayo, M. W., Korneluk, R. G., Goeddel, D. V., and Baldwin, A. S., Jr. (1998) *Science 281*, 1680−1683.
64. Kehry, M. R., and Castle, B. E. (1994) *Semin. Immunol. 6*, 287−294.

BI9909905